Hindawi Publishing Corporation
Advances in Materials Science and Engineering
Volume 2014, Article ID 170148, 7 pages
http://dx.doi.org/10.1155/2014/170148

Research Article

Photocatalytic Degradation of Methylene Blue Using TiO_2 Impregnated Diatomite

Ranfang Zuo,[1] Gaoxiang Du,[1] Weiwei Zhang,[1] Lianhua Liu,[1] Yanming Liu,[1] Lefu Mei,[1] and Zhaohui Li[2]

[1] *School of Material Science and Technology, China University of Geosciences, Beijing 100083, China*
[2] *Geosciences Department, University of Wisconsin-Parkside, Kenosha, WI 53144, USA*

Correspondence should be addressed to Gaoxiang Du; dgx@cugb.edu.cn and Zhaohui Li; li@uwp.edu

Received 6 March 2014; Accepted 12 May 2014; Published 11 June 2014

Academic Editor: Hanlie Hong

Nano-TiO_2 showed a good catalytic activity, but it is easy to agglomerate, resulting in the reduction or even complete loss of photocatalytic activity. The dispersion of TiO_2 particles on porous materials was a potential solution to this problem. Diatomite has high specific surface and absorbability because of its particular shell structure. Thus, TiO_2/diatomite composite, prepared by loading TiO_2 on the surface of diatomite, was a good photocatalyst, through absorbing organic compounds with diatomite and degrading them with TiO_2. Scanning electron microscopy (SEM), energy dispersive spectrum (EDS), X-ray diffraction (XRD), chemical analysis, and Fourier transform infrared spectrometry (FTIR) indicated that TiO_2 was impregnated well on the surface of diatomite. Furthermore, TiO_2/diatomite was more active than nano-TiO_2 for the degradation of methylene blue (MB) in solution. MB at concentrations of 15 and 35 ppm can be completely degraded in 20 and 40 min, respectively.

1. Introduction

With the progression of global industrialization, environmental pollution becomes a more serious issue and, thus, has received considerable attention. The treatment of colored wastewaters produced by the textile industry has recently been heavily researched. Titanium dioxide (TiO_2) is a well-established *n*-type semiconductor used as a photocatalyst to decompose pollutants in water and air as well as produce self-cleaning materials [1, 2]. In recent years, TiO_2 has been widely investigated and used because of its nontoxicity, chemical inertness, high photocatalytic activity, and low cost. TiO_2 has a significant degradation effect as a good photocatalyst of organic and inorganic pollutants in the air and water, which has a broad prospect of application [3].

The photocatalytic activity of TiO_2 is influenced by its crystal structure, particle size, specific surface area, and porosity. Ultrafine powders of TiO_2 show a good catalytic activity. However, agglomeration often takes place, resulting in reduction or even complete loss of photocatalytic activity. The dispersion of TiO_2 particles on porous materials is a potential solution to this problem. Porous materials impregnated with TiO_2 show high thermal stability and larger pore sizes that afford better incorporation of the species without diffusion problems and increased specific surface area [4]. In order to facilitate its recycling and reuse, considerable efforts have been made to load TiO_2 particles on various substrates, such as mica, graphite, glass, diatoms stone, fly-ash, and attapulgite [5, 6]. Diatomite is an important nonmetallic resource with nontoxic and good chemical stability. Diatomite has high specific surface and absorbability because of its particular shell structure [7]. It could serve as an effective substrate for TiO_2 impregnation. This study presents the preparation and characterization of TiO_2-supported diatomite and its photodegradation of methylene blue (MB) in solution.

2. Experimental

2.1. Materials. Diatomite was supplied by Changbai Mountain, Ltd., Jilin Province, China. The medium diameter of diatomite powder, d_{50}, is 34 μm, and the specific surface is

10 m^2/g. Its SiO_2 content was 87%, with other elements, such as Al, Fe, Ca, K, Mg, and Na. Tetrabutyl titanate was obtained from commercially available.

2.2. Preparation of TiO_2/Diatomite Composite. Tetrabutyl titanate was dissolved by ethanol and the solution was gradually added to diatomite. The mixture was stirred for 2 h by magnetic stirrers and then dried in the oven at 80°C. Finally, the dried mixture was further heated to 550°C for about 2 h, before it was cooled naturally. The specific surface of TiO_2/diatomite composite is 32 m^2/g.

2.3. Characterization. The particle size of diatomite powder was measured by a laser particle analyzer Mastersizer 2000. The morphologies of pure diatomite and TiO_2/diatomite composite were examined by scanning electron microscopy (SEM). X-ray diffraction analysis was performed using a D5000 Diffractometer (Siemens) with a Ni filter and CuKα (λ = 1.54 Å) radiation. The UV-Vis absorbance spectra were recorded using Varian Cary 5000. BET surface area was determined at liquid nitrogen temperature (77.3 K) using QUADRASORB SI-MP.

3. Result and Discussion

3.1. The Microstructure and EDS Analysis of Diatomite and TiO_2/Diatomite Composite. Diatomite has porous structure and rough surface after acid treatment (Figure 1(a)). The pore size of diatomite is between 2 and 5 μm. After impregnation, TiO_2 particles formed a dense coating on the surface of the orifice, which presents honeycomb with smaller pore (Figure 1(b)). Compared with raw diatomite, Ti element appeared in the EDS analysis of TiO_2/diatomite composite, indicating that TiO_2 was successfully coated on the surface of diatomite. This result corroborates the high TiO_2 content detected by EDS analysis.

3.2. Chemical Analysis and XRD Patterns. Chemical composition analyses showed that the content of TiO_2 increased from 0.15 to 8.71% after TiO_2 impregnation (Table 1). The result together with that from the EDS analysis indicates that TiO_2 was coated on the surface of diatomite successfully. The reflections of TiO_2 were characteristics of anatase. Diatomite is made of amorphous SiO_2 with only trace amount of quartz. The XRD pattern of TiO_2/diatomite composite revealed mixed phases of anatase TiO_2 and amorphous SiO_2 (Figure 2). The coating of diatomite particles by TiO_2 does not cause any change in their peak positions and shapes compared with the pure TiO_2 and diatomite. The results of XRD analysis and chemical analysis were consistent with that of SEM analysis totally.

3.3. FTIR Analysis. The FTIR spectrum of TiO_2/diatomite composite consists of the characteristic peaks of TiO_2 and diatomite (Figure 3). The band at 1089 cm^{-1} was assigned to the asymmetric stretching vibration modes of Si–O–Si bond [8, 9] and the band at 1633 cm^{-1} was attributed to the stretching mode of O–H bonds on the surface of TiO_2 [10]. The band at 797 cm^{-1} was assigned to the symmetric stretching vibration modes of Si–O bond and the strong absorption peak at 400–600 cm^{-1} was attributed to the vibration mode of Si–O–Ti and Ti–O–Ti bonds [11].

3.4. Adsorption of MB on Different Catalysts and Characterization of Photocatalytic Activity. TiO_2 almost had no adsorption as well as no photocatalyst for MB and the adsorption of TiO_2/diatomite on MB was much lower than pure diatomite for MB (Figure 4). The adsorption reached equilibrium after 30 min in dark. Under dark conditions, TiO_2/diatomite composite removed more MB in comparison to TiO_2 and control, showing almost no activity as well as no photocatalyst for TiO_2 and the control (Figure 5), agreeable to the results presented in Figure 4. In the presence of UV, the rate of MB degradation by TiO_2/diatomite composite was higher than that by TiO_2, attributing to its high surface area and high adsorbability. The MB at concentrations 15 and 35 ppm could be completely degraded after irradiating 20 and 40 min, respectively. The control had the lowest MB self-degradation under UV light. The photoactivity of TiO_2 loaded on diatomite was evidently increased because the high surface area of diatomite effectively concentrates MB around the deposited TiO_2 and produces high concentrations of organic compounds for the TiO_2 photocatalysis. The diatomite might improve the thermal stability of TiO_2 and the surface area and preserve a higher content of surface hydroxyl groups [12].

3.5. UV-Vis Absorption Analysis of MB Solution. Two major absorbance peaks of methylene blue were located at 292 and 664 nm, due to benzene ring and heteropolyaromatic linkage (Figure 6). In addition, the aqueous solution of MB molecules exhibited a double-peak feature at 664 and 615 nm, which correspond to monomers and dimers, respectively [13]. Upon irradiation, the peak at 664 nm has a progressively blue shift to shorter wavelength (Figure 6(b)) because of hypsochromic effect [14, 15]. The absorbance of MB solution was about 2.5 a.u. at time zero. In the presence of TiO_2 the absorbance of MB remained the same after 30 min (Figure 6(a)), agreeing well with the results in Figure 5, while the absorbance of MB decreased sharply after 30 min in the presence of TiO_2/diatomite composite, indicating that TiO_2/diatomite composite has good adsorbability (Figure 6(b)). The absorption peak at 615 nm becomes higher than the peak at 664 nm after 30 min, indicating that the degradation rate of monomers is much higher than that of dimers [14]. Besides, a parallel decrease in intensities and slight blue shift of the bands located at 664 nm also could be observed. These are caused by the N-demethylated degradation concomitantly with the degradation of the phenothiazine [16], as shown in Figure 6(a). And MB was degraded completely after irradiating 60 min and 20 min by TiO_2 and TiO_2/diatomite composite, respectively.

3.6. Mechanism of TiO_2 Activation with UV Light and Photosensitized Oxidation for MB and Its Identification of Intermediate Products. The electron and the hole are generated

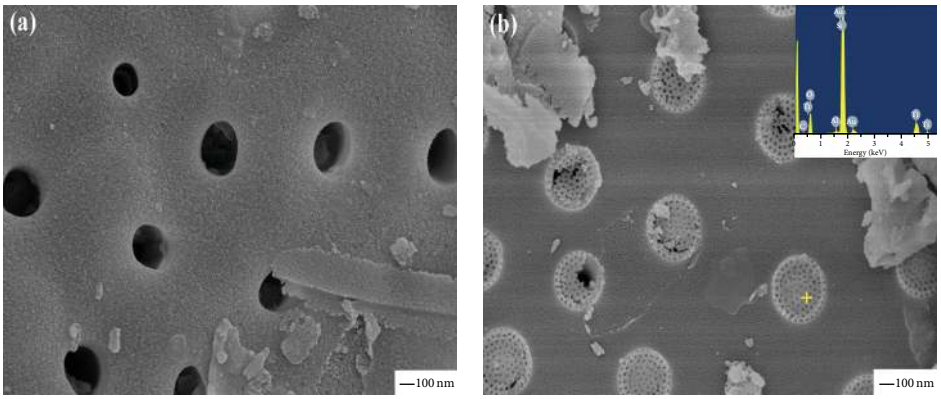

(a) (b)

Figure 1: The microstructure of diatomite and TiO_2/diatomite composite.

Table 1: Chemical analyses of diatomite and TiO_2/diatomite composite.

Composition %	SiO_2	Al_2O_3	Fe_2O_3	MnO	MgO	CaO	Na_2O	K_2O	H_2O^-	TiO_2	P_2O_5
Diatomite	86.82	3.21	1.60	0.011	0.43	0.46	0.25	0.56	0.011	0.15	0.22
TiO_2/diatomite	84.66	2.22	0.61	0.15	1.31	0.23	0.15	0.33	0.45	8.71	0.012

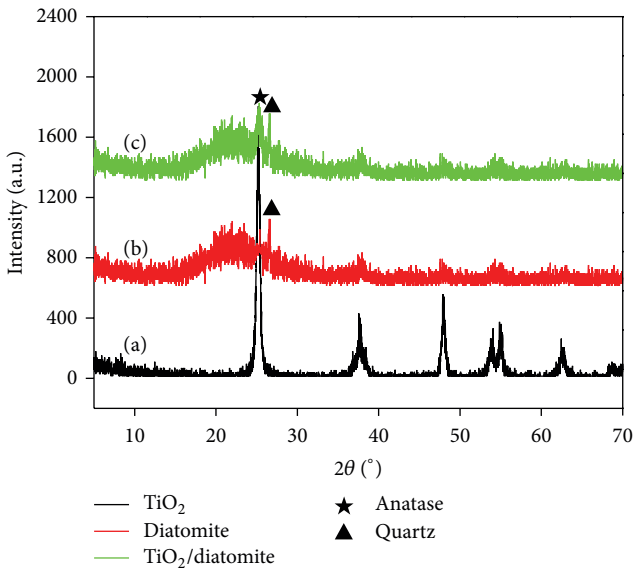

Figure 2: XRD patterns of TiO_2 (a), diatomite (b), and TiO_2/diatomite composite (c).

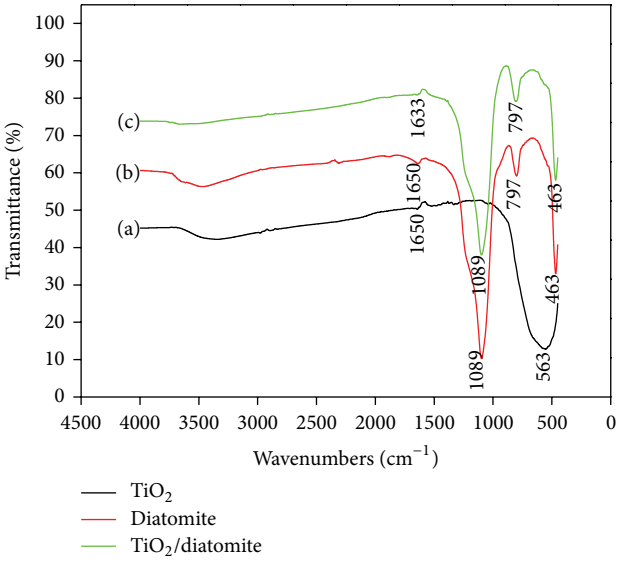

Figure 3: FTIR spectra of TiO_2 (a), diatomite (b), and TiO_2/diatomite composite (c).

in the conduction band and in the valence band of TiO_2 by UV irradiation, respectively, as shown in (A1) [17]. The positive hole can oxidize hydroxide ions (or water molecule) adsorbed on the surface of TiO_2 particles to produce hydroxyl radical [18], as presented in (A2) and (A3) [17]. The electrons of conduction band can react with the oxygen to produce superoxide radical anions (A4) [19]. The superoxide radical anion reacts with a proton to form hydroperoxyl radical (A5):

$$TiO_2 + h\nu\,(\mathrm{UV}) \longrightarrow TiO_2\left(e^-_{CB} + h^+_{VB}\right) \quad (A1)$$

$$TiO_2\left(h^+_{VB}\right) + H_2O \longrightarrow TiO_2 + H^+ + OH^\bullet \quad (A2)$$

$$TiO_2\left(h^+_{VB}\right) + OH^- \longrightarrow TiO_2 + OH^\bullet \quad (A3)$$

$$TiO_2\left(e^-_{CB}\right) + O_2 \longrightarrow TiO_2 + O_2{}^{\bullet-} \quad (A4)$$

$$O_2{}^{\bullet-} + H^+ \longrightarrow HO_2 \quad (A5)$$

For the mechanism of photosensitized oxidation, in the presence of catalysts the excited state of MB injects an electron into the conduction band (B1). The MB dye is then converted to a cationic dye radical that undergoes degradation to yield products according to (B2) to (B5) [17].

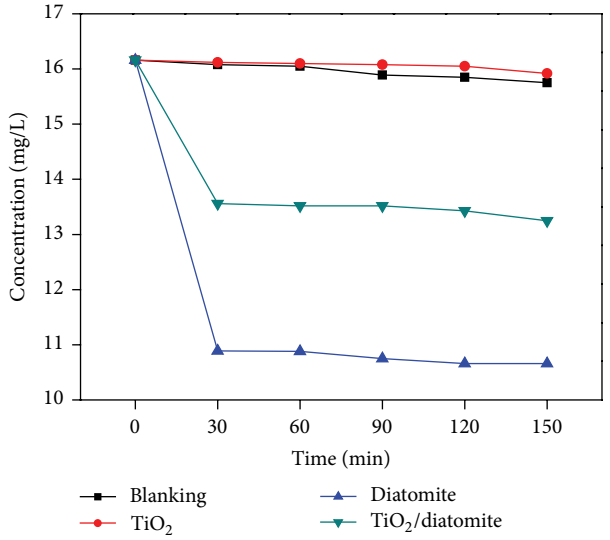

Figure 4: Removal of MB by different sorbents due to adsorption.

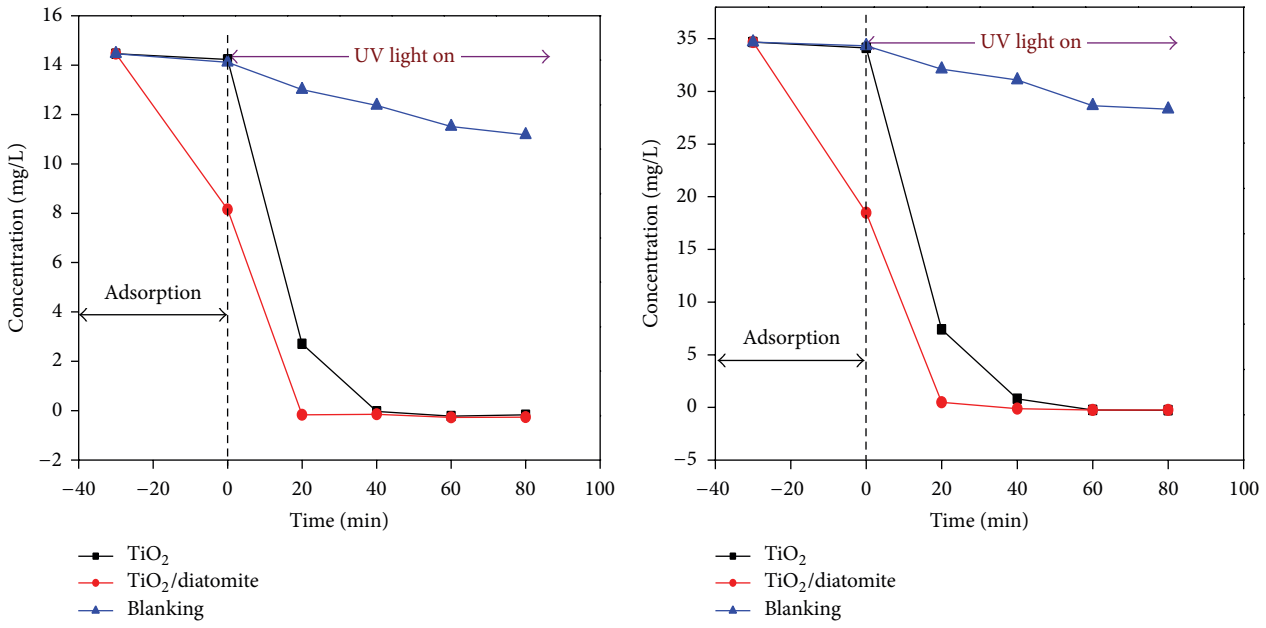

Figure 5: Kinetics of photocatalytic MB degradation from initial MB concentrations of 15 (a) and 35 mg/L (b).

The hydroxyl radical existing on the surface of diatomite accelerated the degradation of MB (B3):

$$MB^{*} + TiO_2 \longrightarrow MB^{\bullet+} e^{-}_{CB} (TiO_2) \quad (B1)$$

$$O_2 + e^{-} \longrightarrow O_2^{\bullet-} \quad (B2)$$

$$MB^{\bullet+} + OH^{-} \longrightarrow MB + OH^{\bullet} \quad (B3)$$

$$MB^{\bullet+} + OH^{\bullet} \longrightarrow \text{products} \quad (B4)$$

$$MB^{\bullet+} + O_2^{\bullet-} \longrightarrow \text{products} \quad (B5)$$

The typical HPLC chromatograms of MB degraded by TiO_2/diatomite under UV light were shown in Figure 7. HPLC analyses showed no degradation products of MB under the condition of adsorption (Figure 7(a)). The decrease in peak height was just caused by adsorption of MB on TiO_2/diatomite (Figure 7(b)). However, the adsorption of the dye molecules over the TiO_2 surface directly affects the occurrence of electron transfer between the excited dye and TiO_2 which further accelerated the degradation rate [20]. In the inserts, peak number 1 represented the retention time of MB, peak number 2 was the self-degradation intermediate metabolite of MB, while peaks number 3 and 4 were further

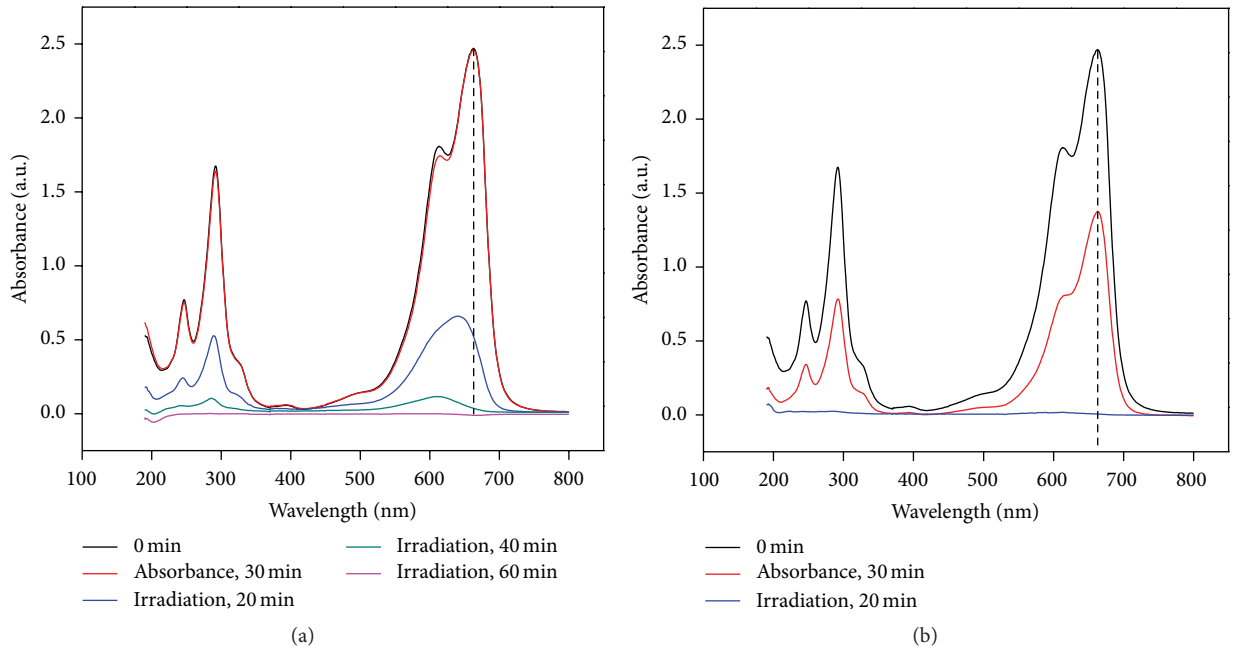

Figure 6: UV absorption spectra of MB solution after reacting with TiO_2 (a) or TiO_2/diatomite composite (b) at different time.

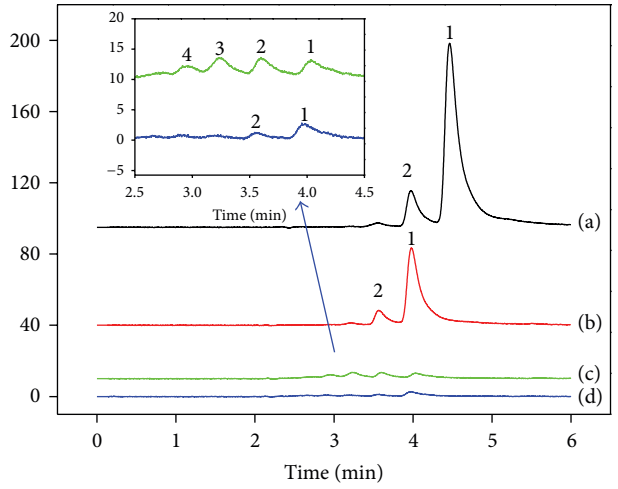

Figure 7: HPLC analyses of MB. (a) Initial MB solution at 15 ppm, (b) equilibrium MB solution after 30 min absorption in the dark, (c) after UV irradiation for 5 min, and (d) after irradiation for 20 min.

degradation products of MB (Figure 7(c)). Peaks number 3 and 4 were further degraded to CO_2 completely in addition to further reduction of peak height of peaks number 1 and 2 after UV irradiation for 20 min. These results are in agreement with the results shown in Figures 5 and 6(b). The MB and its progressive degradation products corresponding to the peaks of 1, 2, 3, and 4 were reported in Scheme 1. The $OH^{\bullet}$ radicals can attack the $C–S^{+}=C$ functional group in MB, which is in direct Coulombic interaction with the surface of TiO_2/diatomite. Therefore, the initial step of MB degradation can be ascribed to the cleavage of the bonds of the $C–S^{+}=C$ functional group in MB. The passage from $C–S^{+}=C$ to C–S(=O)–C requires the conservation of the double bond conjugation, which induces the opening of the central aromatic ring containing both heteroatoms, S and N. The origin of H atoms necessary to C–H and N–H bond formation can be proposed from the proton reduction by photo-generated [21].

4. Conclusion

Impregnation of diatomite with TiO_2 yielded supported anatase catalyst for MB photodegradation. The diatomite supported anatase catalysts were more active than the nano-TiO_2, probably due to the adsorption of MB on diatomite

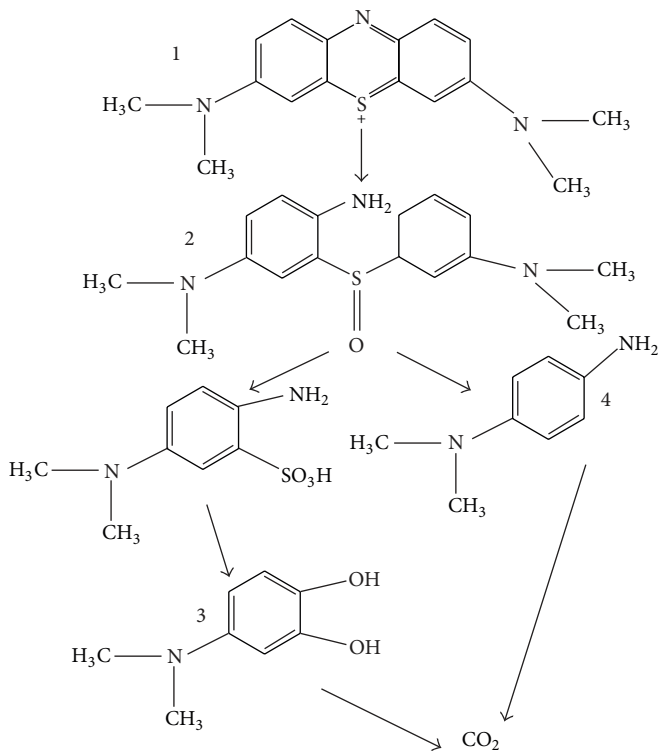

Scheme 1: Photocatalytic degradation pathway of MB.

and the hydroxyl radicals existing on its surface, which accelerated the degradation of MB. At an initial concentration of 15 ppm MB can be completely degraded in 20 min. The results demonstrate that TiO_2/diatomite photocatalysis is a good candidate for color removal in wastewater treatment.

Highlights

(1) Diatomite has high specific surface and absorbability.

(2) The TiO_2/diatomite facilitates the recycling and reuse of TiO_2.

(3) TiO_2/diatomite adsorbs organic compounds with diatomite and degrades them with TiO_2.

Conflict of Interests

The authors declare that there is no conflict of interests regarding the publication of this paper.

Acknowledgment

This work was supported by the Fundamental Research Funds for the Central Universities (no. 2652013037 and no. 2652013043).

References

[1] H. Choi, S. R. Al-Abed, D. D. Dionysiou, E. Stathatos, and P. Lianos, "TiO_2-based advanced oxidation nanotechnologies for water purification and reuse," *Sustainability Science and Engineering*, vol. 8, pp. 229–254, 2010.

[2] D.-J. Kim, H.-C. Pham, D.-W. Park, and K.-S. Kim, "Preparation of TiO_2 thin films on polypropylene beads by a rotating PCVD process and its application to organic pollutant removal," *Chemical Engineering Journal*, vol. 167, no. 1, pp. 308–313, 2011.

[3] W. Mekprasart and W. Pecharapa, "Synthesis and characterization of nitrogen-doped TiO_2 and its photo-catalytic activity enhancement under visible light," in *Proceedings of the Eco-Energy and Materials Science and Engineering Symposium*, vol. 9, pp. 509–514, 2011.

[4] C. Suwanchawalit and S. Wongnawa, "Influence of calcination on the microstructures and photocatalytic activity of potassium oxalate-doped TiO_2 powders," *Applied Catalysis A*, vol. 338, no. 1-2, pp. 87–99, 2008.

[5] P. Huo, Y. Yan, S. Li, H. Li, and W. Huang, "Preparation of poly-o-phenylenediamine/TiO_2/fly-ash cenospheres and its photodegradation property on antibiotics," *Applied Surface Science*, vol. 256, no. 11, pp. 3380–3385, 2010.

[6] S. Zhou, J. Lv, L. K. Guo et al., "Preparation and photocatalytic properties of N-doped nano-TiO_2/muscovite composites," *Applied Surface Science*, vol. 258, no. 16, pp. 6136–6141, 2012.

[7] G. X. Du, R. F. Zuo, L. F. Mei, J. H. Liao, and W. J. Guo, "Surface modification of diatomite by silane coupling agent and its effect

on the reinforcing efficiency of NB/SBR blend," *Rare Metal Materials and Engineering*, vol. 42, pp. 412–417, 2013 (Chinese).

[8] Y. Liu, C. Ge, M. Ren et al., "Effects of coating parameters on the morphology of SiO_2-coated TiO_2 and the pigmentary properties," *Applied Surface Science*, vol. 254, no. 9, pp. 2809–2819, 2008.

[9] Y. Zhang, H. Yin, A. Wang et al., "Deposition and characterization of binary Al_2O_3/SiO_2 coating layers on the surfaces of rutile TiO_2 and the pigmentary properties," *Applied Surface Science*, vol. 257, no. 4, pp. 1351–1360, 2010.

[10] H.-X. Guo, K.-L. Lin, Z.-S. Zheng, F.-B. Xiao, and S.-X. Li, "Sulfanilic acid-modified P25 TiO_2 nanoparticles with improved photocatalytic degradation on Congo red under visible light," *Dyes and Pigments*, vol. 92, no. 3, pp. 1278–1284, 2012.

[11] X. F. Hou, H. Ding, Y. X. Zheng, and M. M. Wang, "Preparation and characterisation of amorphous silica/anatase composite through mechanochemical method," *Materials Research Innovations*, vol. 17, pp. 234–239, 2013.

[12] X. Wang, Z. Hu, Y. Chen, G. Zhao, Y. Liu, and Z. Wen, "A novel approach towards high-performance composite photocatalyst of TiO_2 deposited on activated carbon," *Applied Surface Science*, vol. 255, no. 7, pp. 3953–3958, 2009.

[13] C. An, S. Peng, and Y. Sun, "Facile synthesis of sunlight-driven AgCl:Ag plasmonic nanophotocatalyst," *Advanced Materials*, vol. 22, no. 23, pp. 2570–2574, 2010.

[14] F.-T. Li, Y. Zhao, Y. Liu, Y.-J. Hao, R.-H. Liu, and D.-S. Zhao, "Solution combustion synthesis and visible light-induced photocatalytic activity of mixed amorphous and crystalline $MgAl_2O_4$ nanopowders," *Chemical Engineering Journal*, vol. 173, no. 3, pp. 750–759, 2011.

[15] N. C. Castillo, A. Heel, T. Graule, and C. Pulgarin, "Flame-assisted synthesis of nanoscale, amorphous and crystalline, spherical $BiVO_4$ with visible-light photocatalytic activity," *Applied Catalysis B*, vol. 95, no. 3-4, pp. 335–347, 2010.

[16] F. Wang, S. Min, Y. Han, and L. Feng, "Visible-light-induced photocatalytic degradation of methylene blue with polyaniline-sensitized TiO_2 composite photocatalysts," *Superlattices and Microstructures*, vol. 48, no. 2, pp. 170–180, 2010.

[17] H. A. Le, L. T. Linh, S. Chin, and J. Jurng, "Photocatalytic degradation of methylene blue by a combination of TiO_2-anatase and coconut shell activated carbon," *Powder Technology*, vol. 225, pp. 167–175, 2012.

[18] R.-J. Wu, C.-C. Chen, C.-S. Lu, P.-Y. Hsu, and M.-H. Chen, "Phorate degradation by TiO_2 photocatalysis: parameter and reaction pathway investigations," *Desalination*, vol. 250, no. 3, pp. 869–875, 2010.

[19] G. Wang, F. Wu, X. Zhang, M. Luo, and N. Deng, "Enhanced TiO_2 photocatalytic degradation of bisphenol E by β-cyclodextrin in suspended solutions," *Journal of Hazardous Materials*, vol. 133, no. 1–3, pp. 85–91, 2006.

[20] K. Natarajan, T. S. Natarajan, H. C. Bajaj, and R. J. Tayade, "Photocatalytic reactor based on UV-LED/TiO_2 coated quartz tube for degradation of dyes," *Chemical Engineering Journal*, vol. 178, pp. 40–49, 2011.

[21] A. Houas, H. Lachheb, M. Ksibi, E. Elaloui, C. Guillard, and J.-M. Herrmann, "Photocatalytic degradation pathway of methylene blue in water," *Applied Catalysis B*, vol. 31, no. 2, pp. 145–157, 2001.